THE JOURNAL OF PHYSICAL CHEMISTRY B

Article

pubs.acs.org/JPCB

Self-Association and Complexation of the Anti-Cancer Drug Doxorubicin with PEGylated Hyperbranched Polyesters in an Aqueous Environment

K. Karatasos*

Physical Chemistry Laboratory, Chemical Engineering Department, Aristotle University of Thessaloniki, 54124 Thessaloniki, Greece

Supporting Information

ABSTRACT: Fully atomistic molecular dynamics simulations were employed in order to examine in detail the self-assembly characteristics and the complexation behavior of the anticancer drug doxorubicin with PEGylated hyperbranched polyesters in an aqueous environment. We have examined two variants of the polymeric compound by altering the length of the hydrophilic poly(ethylene glycol) arms attached to the hydrophobic hyperbranched core. By comparing the clustering properties of the drug molecules in a polymer-free system to those in the polymer-containing models, we were able to assess the effects related to the presence and to the structural features of the polymer moiety. In addition, we have distinguished the effects associated with the neutral and protonated drug molecules separately. It was found that, in the presence of the polymeric material, the drug molecules formed clusters preferentially close to the polymer's periphery, the characteristics of which depended on the structural details of the polymeric host and on the charge of the drug molecules. Hydrogen bonding was found to contribute to the polymer/drug complexation, with the nature of the prevailing donor/acceptor pairs depending on the charge of the drug. Dynamic analysis of the drugs' motion revealed that in the polymer-containing systems the drug molecules experienced a larger degree of confinement within the formed clusters compared to that describing their polymer-free analogues, while the structural coherence of the clusters was found to be more persistent in the system with the larger poly(ethylene glycol) arms. The results described in this work, through the monitoring of both static and dynamic aspects of the self-association and the complexation behavior of the neutral and charged molecules of doxorubicin with the polymeric host, may help toward the elucidation of the key parameters that are involved in the formation of effective polymer-based carriers for drug molecules of the anthracycline family used in cancer chemotherapy.

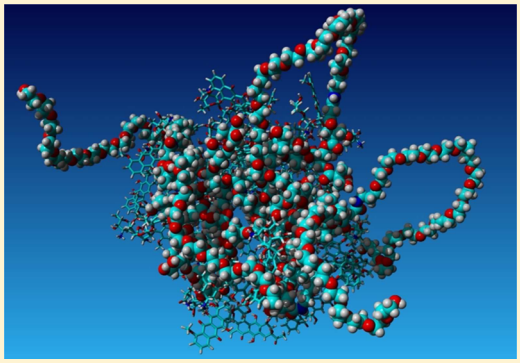

I. INTRODUCTION

In recent years, a new category of multifunctional biocompatible materials, i.e., hyperbranched polymers, possessing unique physicochemical and rheological properties, have emerged as promising nanocarriers for drug and gene delivery purposes.[1,2] One of the families of such multibranched polymeric materials which have been studied experimentally as well as computationally[3−5] are those bearing a perfect dendritic topology (commonly referred to as dendrimers) which starts from a central core and grows radially outward in a systematic manner. Although significant progress has been made in their utilization as vehicles for biopharmaceutical substances, their widespread use has been hampered by the high cost related to their synthesis. To this direction, nonregularly branched polymers can be considered as cost-effective alternatives of dendrimers.[6,7] These polymers retain the highly desirable attributes of dendrimers (such as the nanoscale dimensions and multifunctionality), and they can be produced in large quantities via one-step synthetic protocols.[8] In this context, there is a growing interest to produce new formulations based on these hyperbranched polymers as carriers for drugs and genetic material.[7,9,10]

One of the main obstacles that has to be surmounted toward a wider use of some common categories of hyperbranched polymers (such as hyperbranched polyesters[11]) is their poor solubility in an aqueous environment. To remedy this problem, novel chemistry protocols have been developed which address this issue by proper functionalization of these molecules, rendering them water-soluble and thus increasing their potential to act as effective agents for drug and gene delivery applications.[12,13] In addition, this strategy (e.g., PEGylation of poorly water-soluble hyperbranched polymers) has been shown to provide an efficient route toward a better control of the physical properties of these polymeric materials[14,15] which can be exploited in processes related to their biomedical usage.[16] In the present work, we have simulated a member of the family of hyperbranched polyesters (commercially available as Boltorn[17]) functionalized with linear poly(ethylene glycol) (PEG) segments—which render the polymer water-soluble—as a potential complexation agent for the drug doxorubicin

Received: December 10, 2012
Revised: January 28, 2013
Published: February 4, 2013

   dx.doi.org/10.1021/jp312125c | J. Phys. Chem. B 2013, 117, 2564−2575

Scheme 1. The Structure of the Hydrophobic Hyperbranched Core (Left) and of the Neutral Doxorubicin Molecule (Right)

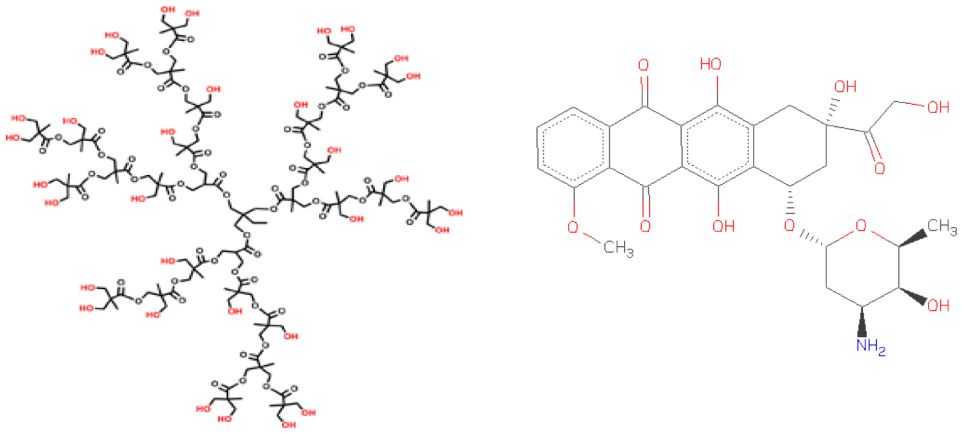

(DOX) (Scheme 1), which is commonly used in cancer chemotherapy treatments.[18,19] Common issues that have arisen by its use relate to the level of cytotoxicity against normal cells, its limited solubility in water, as well as its low bioavailability.[20,21] Efforts toward remedying such problems have been made by complexation of DOX with hyperbranched polymers via exploitation of the structural properties of these systems as well as of certain favorable interactions (i.e., hydrophobic, hydrogen bonding) that can be regulated in order to enhance the loading and ultimately the therapeutic action of the drug molecules.[22,23]

The particular system that we have examined (i.e., the PEGylated hyperbranched polyesters) has very recently been chemically synthesized, and initial experiments have already been conducted exploring the possibilities for complex formation with doxorubicin.[23] Motivated by the encouraging results of these proof-of-concept experiments and the emerging prospects of a wider utilization of these amphiphilic polymers as vectors for DOX or other similar drugs, we aimed at elucidating details on the associative behavior of the drug molecules in the presence of the polymeric compound, by performing fully atomistic molecular dynamics (MD) simulations. A better understanding of the parameters (i.e, spatial confinement, specific interactions, structural details of the polymer host, etc.), which may promote the polymer/drug complexation and contribute to the structural stability of the formed complexes, is expected to offer a valuable insight toward the production of such complexes with improved efficacy.

II. DESCRIPTION OF THE EXAMINED MODELS AND SIMULATION DETAILS

The hydrophobic core of the polymeric particles is comprised by a hyperbranched polyester bearing the commercial name Boltorn H30[11] (Scheme 1).

Hyperbranched polymers of this family are biocompatible and biodegradable and have already been found to exhibit favorable binding and release properties of drug molecules.[24−27] The H30 core of the host nanoparticle is decorated with five PEG arms (a PEG segment is attached to every other terminal branch). In one of the systems (termed as H30PEO20 henceforth), each PEG arm consists of 20 monomers, while in the other (referred to as H30PEO40 henceforth) the PEG segment is 40 monomers in length. The chemical joints between H30 and the PEG arms are modeled exactly as in the actual molecule (more details can be found in ref 23).

Figure 1 shows the H30-cored PEGylated polymers before addition of the drug polymers, the counterions, and the solvent (water).

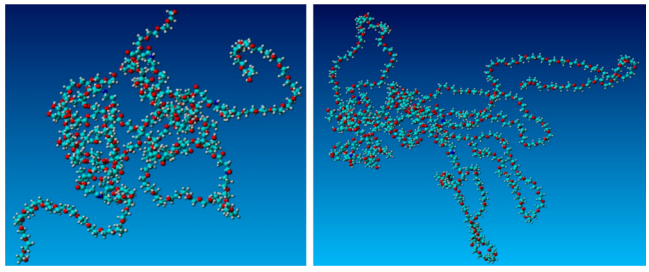

Figure 1. The H30PEO20 (left) and H30PEO40 (right) nanoparticles.

For the drug molecules, we have included a mixture of neutral and protonated DOX in our models, since, as has been found in relevant experiments, in physiological pH, DOX is partially ionized after protonation of the amine group.[28] The percentage of the protonated drug molecules was calculated via the Henderson−Hasselbalch relation[29] (eq 1) by taking into account the pK_a at 37 °C and in an ionic strength of 165 mM:[30]

$$N_{\text{charged}} = \frac{10^{\text{p}K_a - \text{pH}}}{1 + 10^{\text{p}K_a - \text{pH}}} N_{\text{total}} \quad (1)$$

In eq 1, N_{charged} refers to the number of protonated DOX molecules and N_{total} to the total number of drug molecules.

To stay close to experimental conditions, we have performed the simulations at the same temperature (T = 310 K) and ionic strength (I = 0.165 M) (including the appropriate number of Na^+ and Cl^- counterions) as those in which the pK_a of DOX was determined. The initial structure of the H30 core was taken from a previous work,[31] while for doxorubicin the initial structure was the same as in ref 32. The energetic parameters were adopted from the GAFF force field[33] which is an extension of the AMBER[34] set of parameters. This parametrization is consistent with those used in past studies for the hyperbranched polyesters[31,35] doxorubicin[32,36] and PEG.[37] Water molecules were parametrized using the TIP3P model[38] which has already been used in the description of aqueous solutions of PEG[37,39] and DOX.[32] As in the relevant experimental work,[23] we have kept the weight ratio between the drug molecules and the polymeric host close to 3 w/w %. In

dx.doi.org/10.1021/jp312125c | J. Phys. Chem. B 2013, 117, 2564−2575

Table 1. Details of the Simulated Models

model	no. of protonated DOX molecules	no. of neutral DOX molecules	no. of water molecules	no. of Na^+	no. of Cl^-	ratio drug/carrier (w/w %)
H30PEO20	31	19	44 223	121	152	3.1
H30PEO40	45	28	76 772	214	259	3.0
DOX31p19n	31	19	40 850	111	142	

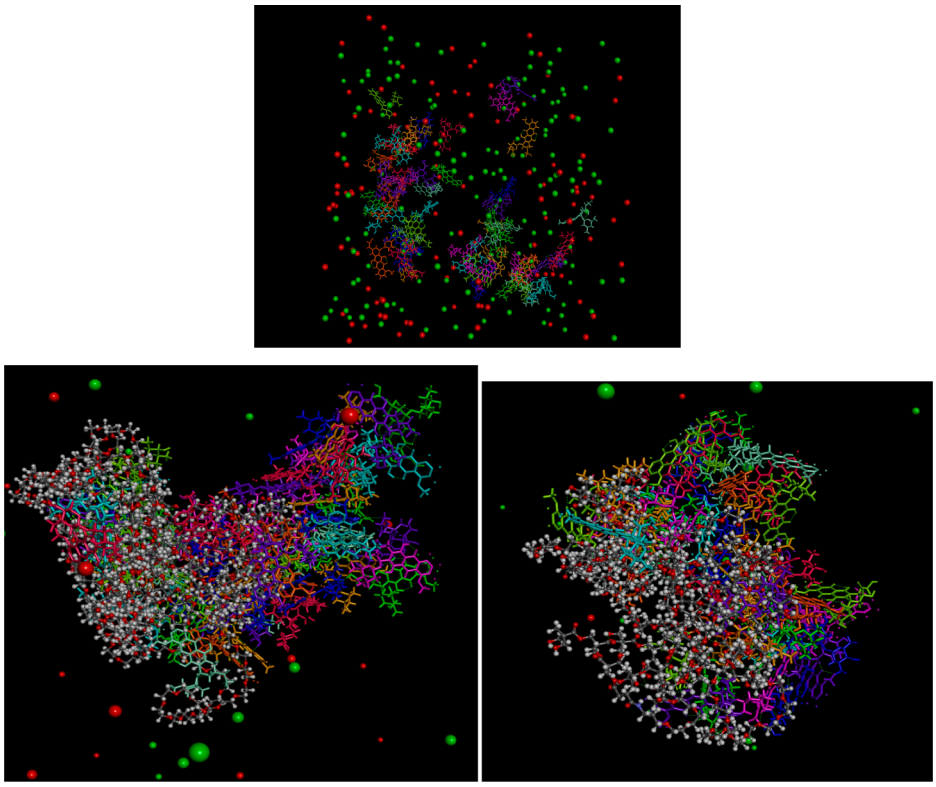

Figure 2. The upper panel shows a snapshot of the DOX31p19n after equilibration. The lower panel shows equilibrated models of H30PEO40 (left) and H30PEO20 (right). DOX molecules appear in stick representation (each with a different color in the color version), the polymer nanoparticles appear in ball and stick form, and the Na^+ and Cl^- are shown as red and green beads, respectively. Water molecules are omitted for clarity. Only a zoomed-in part of the simulation boxes is displayed.

addition, in order to simulate appropriate hydration conditions, we have constructed the simulation box so that in the initial configuration a water layer of at least 15 Å thickness surrounded any solute molecules in all directions.

For comparison purposes, we have also simulated an aqueous solution of doxorubicin molecules (referred to as DOX31p19n) keeping the experimental percentage of protonation of the amine group, at the same temperature and ionic strength and at the same overall weight fraction of DOX in the solution, as in the H30PEO20 and H30PEO40 systems. Details for the composition of the examined systems are given in Table 1.

At the initial stage of the construction of the H30PEO20 and H30PEO40 models, DOX molecules were placed within a spherical shell of width moderately larger compared to the radius of gyration of the polymeric host. Next, the so-constructed initial configurations were solvated with pre-equilibrated TIP3P water molecules[40] as described above. A suitable number of Na^+ and Cl^- counterions was then added to neutralize the system and to set the ionic strength level. For the DOX31p19n system, the DOX molecules were solvated with an appropriate number of TIP3P waters and counterions, so that the same conditions of ionic strength and overall drug weight fraction as in the H30PEO systems were met.

Ensuing the construction, the systems were subjected in an annealing procedure which included successive stages of heating by 50 K steps each time up to 700 K and then cooling down to 300 K at constant volume conditions. Finally, the systems were brought to the target temperature of 310 K. At each temperature during the annealing procedure, a combination of steepest descent and conjugate gradient energy minimization was performed, which was followed by 50 ps of MD at constant volume and temperature conditions. After the target temperature was reached, the systems were again subjected to energy minimization cycles followed by isobaric–isothermal (NPT) MD equilibration steps. During MD equilibration, several energetic components together with static and conformational properties of the solutes (e.g., radius of gyration of the polymeric host, average distance between the polymer and the drug molecules, and distribution of water molecules and counterions around the PEGylated polyester) were monitored, to ensure their stabilization prior to the commencement of the production runs. Figure 2 shows snapshots of the examined systems without the waters, for clarity (see models with water included, in Figure S1 in the Supporting Information).

The length of the equilibration trajectory for the polymer-containing systems exceeded 10 ns before certain conforma-

dx.doi.org/10.1021/jp312125c | J. Phys. Chem. B 2013, 117, 2564–2575

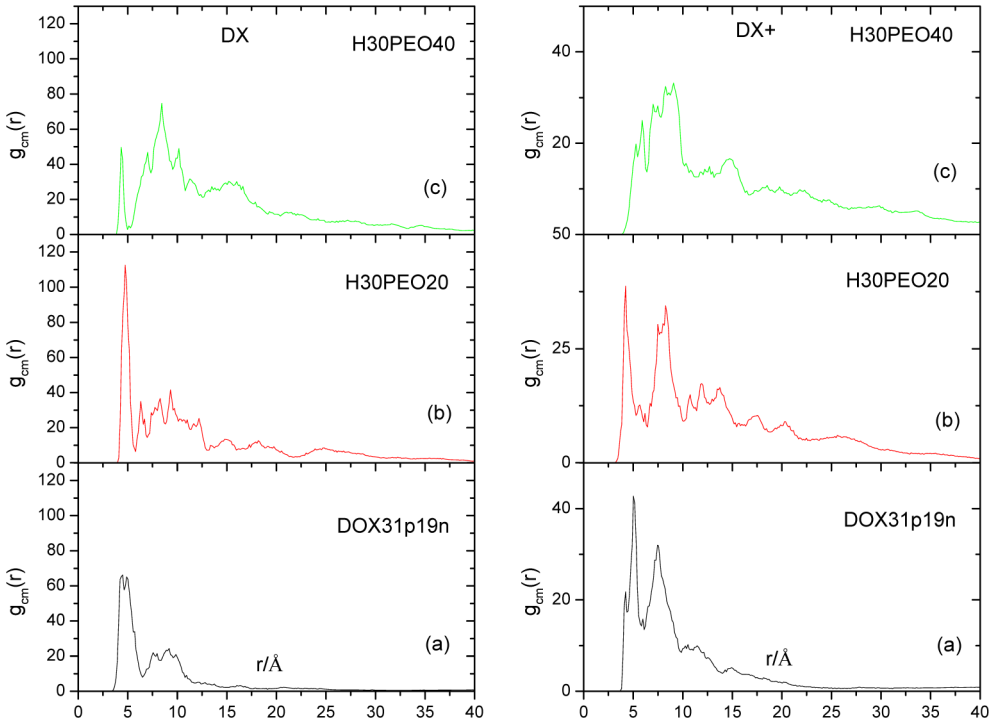

Figure 3. Radial distribution functions of the center of mass of the DOX molecules in the examined systems, for the neutral (left, DX) and the protonated (right, DX+) molecules.

tional characteristics of the polymeric hosts were stabilized (see Figure S2 in the Supporting Information). Ensuing equilibration, MD NPT trajectories (T = 310 K, P = 1 bar) of about 30 ns were generated with 1 fs integration steps and a frame-saving frequency of 1 ps. The Langevin method for the control of temperature (with a damping coefficient of 3 ps^{-1}) and the Nose–Hoover Langevin piston method[41] for the control of pressure (using a piston period of 0.8 ps and a decay time of 0.4 ps) were used for temperature and pressure control, respectively. Electrostatic interactions were computed by means of the particle mesh Ewald (PME) algorithm.[42] All simulations were performed with NAMD 2.8[43] employing periodic boundary conditions and with a distance cutoff at 12 Å.

III. ASSOCIATIVE BEHAVIOR OF DOX MOLECULES

As was noticed in relevant studies,[28,30,44] doxorubicin exhibits a tendency for self-association in aqueous solutions, driven mainly by hydrophobic forces through the π-electron interaction between the planar aromatic portions. This behavior was also noticed in the presence of other compounds of biological or non-biological nature, while it was observed that addition of water-soluble compounds enhanced its associative behavior in the water phase.[30] The trend for self-association of DOX molecules in aqueous solutions is observed in our simulations, as shown in Figure 2. For DOX31p19n, the system reaches a thermodynamic equilibrium through the formation of distinct DOX clusters, while in the presence of the polymeric nanoparticle these clusters appear to form mainly in the vicinity of the PEGylated hyperbranched polyester. Since this behavior may influence the transport properties of the formed complexes and ultimately the drug biodistribution, we have tried to examine in more detail the static as well as dynamic characteristics of the assemblies as described below.

III.1. Static Aspects. To check the changes in the associative behavior between DOX molecules in the presence of the polymeric particle, we have examined the radial distribution function arising from the centers of mass of the drug molecules, as shown in Figure 3.

Before getting into the detailed comparison of the radial distribution functions in the three examined systems, it is worth noticing that there are differences between the pictures describing the neutral (left column, Figure 3) and protonated DOX molecules (right column, Figure 3). The electrostatic repulsions due to the presence of the charged amine groups in the protonated species affect the spatial arrangement of the molecules (i.e., the relative intensity and the number of observed peaks). Focusing now on the behavior in the DOX31p19n system, it appears that the distributions are almost bimodal, characterized by a sharper peak close to an intermolecular distance of 5 Å and a second maximum close to 8 Å. The short-distance peak arises from the closest neighbors of a drug molecule and would be consistent with the formation of dimers, while the peak corresponding to 8 Å could in principle arise either from larger in size drug aggregates (in that case, the second peak would represent intracluster separations) or from neighboring clusters. However, the assignment of the second neighbor peak to the formation of larger clusters is not likely for the polymer-free and H30PEO20 models, as will be discussed in section III.2 later in the text.

Introduction of the short-arm PEGylated polyester (Figure 3b) incurs changes particularly in longer separations between the DOX molecules. The clustering of drug molecules persists and the distances between neighboring molecules or neighboring clusters seem to become well-defined, as implied by the enhancement of the peak near 8 Å and the appearance of several smaller-amplitude maxima at larger separations. The changes with respect to the DOX31p19n systems are more pronounced in the longer-arm PEGylated polyester (Figures

dx.doi.org/10.1021/jp312125c | J. Phys. Chem. B 2013, 117, 2564–2575

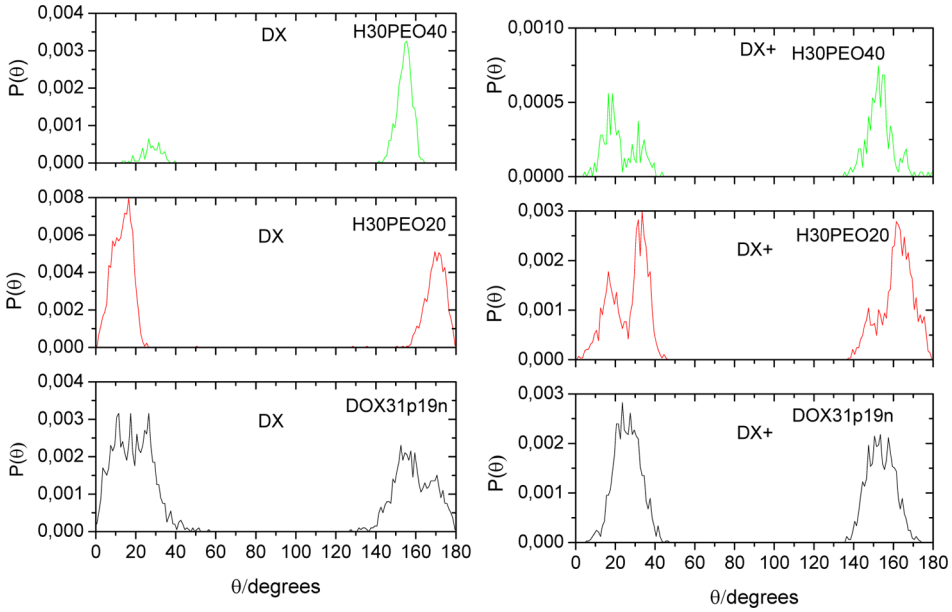

Figure 4. Distributions of the angles between inertia eigenvectors (see text), for DOX molecules with a maximum separation of 5 Å between their centers of mass.

3c) in which the width of the peaks as well as their number and location are distinctly different.

The formation of aggregates by the drug molecules and the structural characteristics of these clusters may be of paramount importance regarding their pharmacological action, since they can influence their transport properties, their permeation through the cellular membrane, and their binding to DNA.[45,46] To elaborate more on the possible effects of the presence of the polymeric compound in the spatial arrangement of the drug molecules within a cluster, we have examined their relative orientation by monitoring the angle between the pertinent principal axes of inertia. To ensure that the obtained distributions describe the orientations of drug molecules belonging in the same cluster, we have only taken into account those molecules for which the separation between their centers of mass did not exceed 5 Å, which corresponds to the location of the first peak of the radial distribution functions shown in Figure 3. The principal axes of rotation were determined via diagonalization of the moment of inertia tensor

$$I = \sum_{i=1}^{N} m_i[(\mathbf{r}_i \times \mathbf{r}_i)\mathbf{l}_3 - (\mathbf{r}_i\mathbf{r}_i^{\mathrm{T}})] \quad (2)$$

where $\mathbf{r}_i$ is the position vector of the ith atom relative to the center of mass of the molecule, N is the number of atoms per molecule, and $\mathbf{l}_3$ is the unitary matrix of the third order. The eigenvectors of the inertia tensor define the directions of the principal axes for each drug molecule. The highest eigenvalue corresponds to the eigenvector along the longer axis of the molecule. The angle between two drug molecules can be calculated through the scalar product of the respective eigenvectors. Figure 4 illustrates the distribution of the angles formed by the unit vectors corresponding to the largest eigenvalue of the inertia tensor. As is readily inferred from the distributions in Figure 4, at all systems, the immediately neighboring DOX molecules practically assume either a parallel (low angles) or an antiparallel (larger angles) placement, in line with relevant NMR experiments.[44]

Certain deviations from this trend are observed in the arrangement of the charged molecules in the presence of the polymeric host. For both cases, though (i.e., either for charged or for neutral drugs), introduction of the polymer compound imparts significant changes in the profiles with respect to those of the polymer-free system. For the neutral drugs (Figure 4, left), the profiles become sharper in the H30PEO20 model, indicating a better alignment of the molecules, while, in the H30PEO40, the peaks characterizing the distributions indicate a larger deviation from a parallel arrangement. In the latter model, the antiparallel placement of the DOX molecules is prevailing. In the profiles characterizing the protonated drugs in the polymer-containing models (Figure 4, right), additional peaks appear (this is more prominent in the "parallel" peaks), indicating two different preferential orientations of the drug molecules in the formed clusters: one peaked at a lower and one peaked at a larger angle with respect to the corresponding polymer-free profiles. Since this differentiation is observed in the "parallel" peaks, the two preferential orientations might be related to different conformations of the sugar group bearing the charged amine. This in turn might be associated with preferred van der Waals, electrostatic, or specific interactions (such as hydrogen bonding which will be discussed later) between the amine groups and the polymeric host.

The intensity of such interactions between the polymeric nanoparticle and the drug clusters or the individual DOX molecules would essentially depend on their proximity and on the relative arrangement of the drug molecules around the polymeric compound. The majority of the drug clusters, as implied by the snapshots of Figure 2 (lower panel), seem to be assembled in the vicinity of the polymer nanoparticle. This notion is corroborated by Figure 5 where the average distance between the centers of mass of the polymeric solute and the DOX molecules is shown.

In both polymer-containing systems, on average, the doxorubicin molecules remain in the vicinity of the polymeric moiety during the entire simulation window. The DOX molecules in the H30PEO40 systems are located on average at a somewhat longer distance compared to their analogues in

dx.doi.org/10.1021/jp312125c | J. Phys. Chem. B 2013, 117, 2564−2575

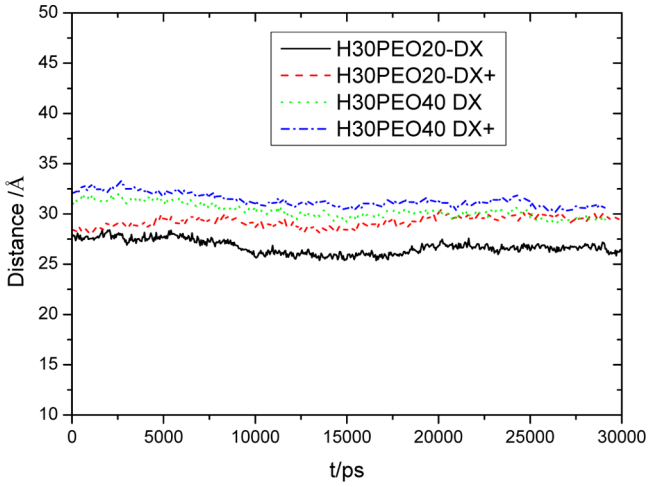

Figure 5. Average distance between the center of mass of the neutral and protonated drug molecules and that of the corresponding PEGylated polyester.

the H30PEO20 model. This can be related to a small difference in the radii of gyration between the polymers in the two systems, i.e., $\langle R_g \rangle \cong 20.7$ Å in the H30PEO40 and $\langle R_g \rangle \cong 17.5$ Å in the H30PEO20 system. In the latter case, the shorter PEG arms would also allow for a better access of the drug molecules to the polyester core and thus to a higher probability of geometric entrapment and/or enthalpic interactions with the hydrophobic core. In both systems, the average distance of DOX molecules from the center of mass of the polymer is almost 50% larger compared to the respective radius of gyration of the latter, indicating that a significant percentage of the drug molecules is located at the periphery of the polymeric structure. A more detailed picture on the manner that the DOX molecules are arranged around the branched polymer can be provided by examining the corresponding distributions. Figure 6 depicts the weight distributions of all the molecular species and the counterions around the center of mass of the polymer nanoparticle.

A visual inspection of the corresponding distributions reveals that, in both systems containing the PEGylated polyester, almost all the drug molecules (i.e., taking into account the distributions of both the neutral and protonated drugs) are arranged within a sphere extending from the center of mass to the periphery of the polymer (i.e., to the distance at which the distribution of the polymer reaches 0). Interestingly, though, the profiles characterizing the charged and neutral DOX molecules exhibit characteristic differences. Namely, the distributions of the neutral drugs are more "discrete" in nature (i.e., there are well-defined distinct peaks) compared to those corresponding to the protonated drug molecules, which exhibit rather broad peaks with a maximum close to twice the radius of gyration of the polymer. In other words, the neutral DOX molecules remain in their majority organized in clusters which are arranged at characteristic distances from the center of mass of the polymer, whereas their protonated analogues are more homogenously distributed throughout the polymeric structure, with a more probable location close to the nanoparticle's periphery. As far as the water molecules are concerned, in both systems, water penetrates well within the polymeric interior.

The differences in the spatial arrangement between the neutral and protonated DOX molecules in the presence of the polymeric host as described above implies that to a certain extent they may be subjected to different (or at least to similar in nature but different in intensity) interactions with the solute or the solvent. Since hydrogen bonding is known to play a significant role in the complexation between hydrogen-bonding-capable drugs and their potential delivery vehicles,[47−49] it is of interest to examine whether the structural differences between the two polymeric hosts studied in this work may affect the hydrogen-bonding behavior of the drug molecules, either between the drug and the polymer or between the drug and water. To this end, we have examined appropriate donor−acceptor pairs by evaluating the corresponding pair correlation functions.

For the detection of a hydrogen bond, we relied on the hydrogen−acceptor distance in combination with the angle formed by the donor−hydrogen−acceptor triplet. The minimum donor−hydrogen−acceptor angle was taken to be 120°.[50,51] The atomic pairs we have examined were the water oxygen (OT) with the amine hydrogens of DOX (HN), as well as pairs formed by hydroxyl oxygens (OH) and carbonyl oxygens (O) with hydroxyl hydrogens (HO) and amine hydrogens (HN). Figure 7 shows such correlation functions for the HN−OT pairs. A peak close to 2 Å distance is indicative for the formation of a hydrogen bond.[52] A cursory glance at the correlation functions in Figure 7 reveals that in the DOX31p19n system hydrogen bonding between doxorubicin and water is much more frequent in protonated molecules. This trend is present in the polymer-containing systems as well. The

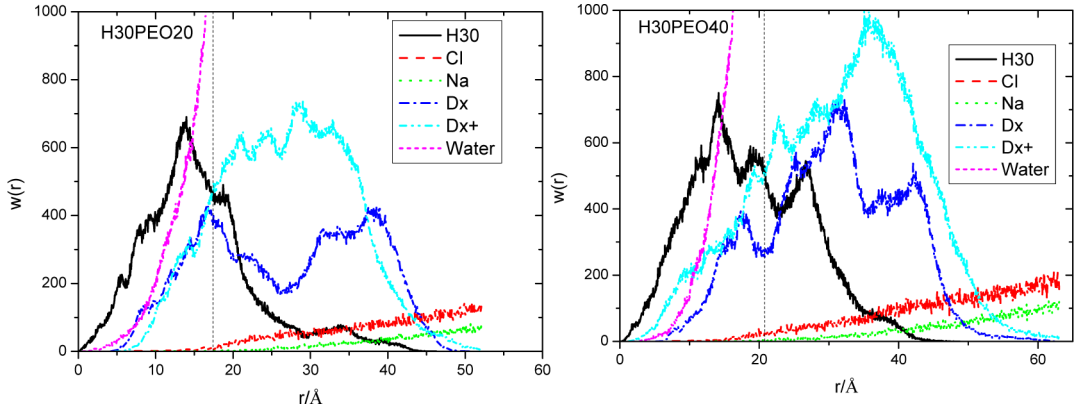

Figure 6. Weight distributions of all the molecular species and the counterions around the center of mass of the polymeric solute. The vertical dashed lines denote the location of the respective radius of gyration of the polymer.

dx.doi.org/10.1021/jp312125c | J. Phys. Chem. B 2013, 117, 2564−2575

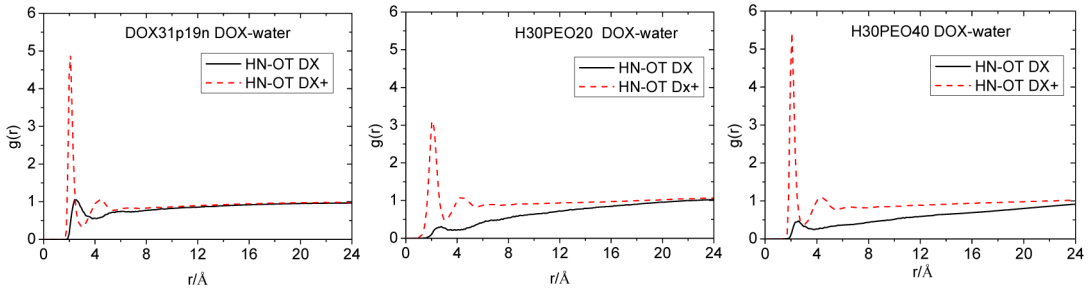

Figure 7. Pair correlation functions between the amine hydrogens of the DOX molecules and the water oxygens.

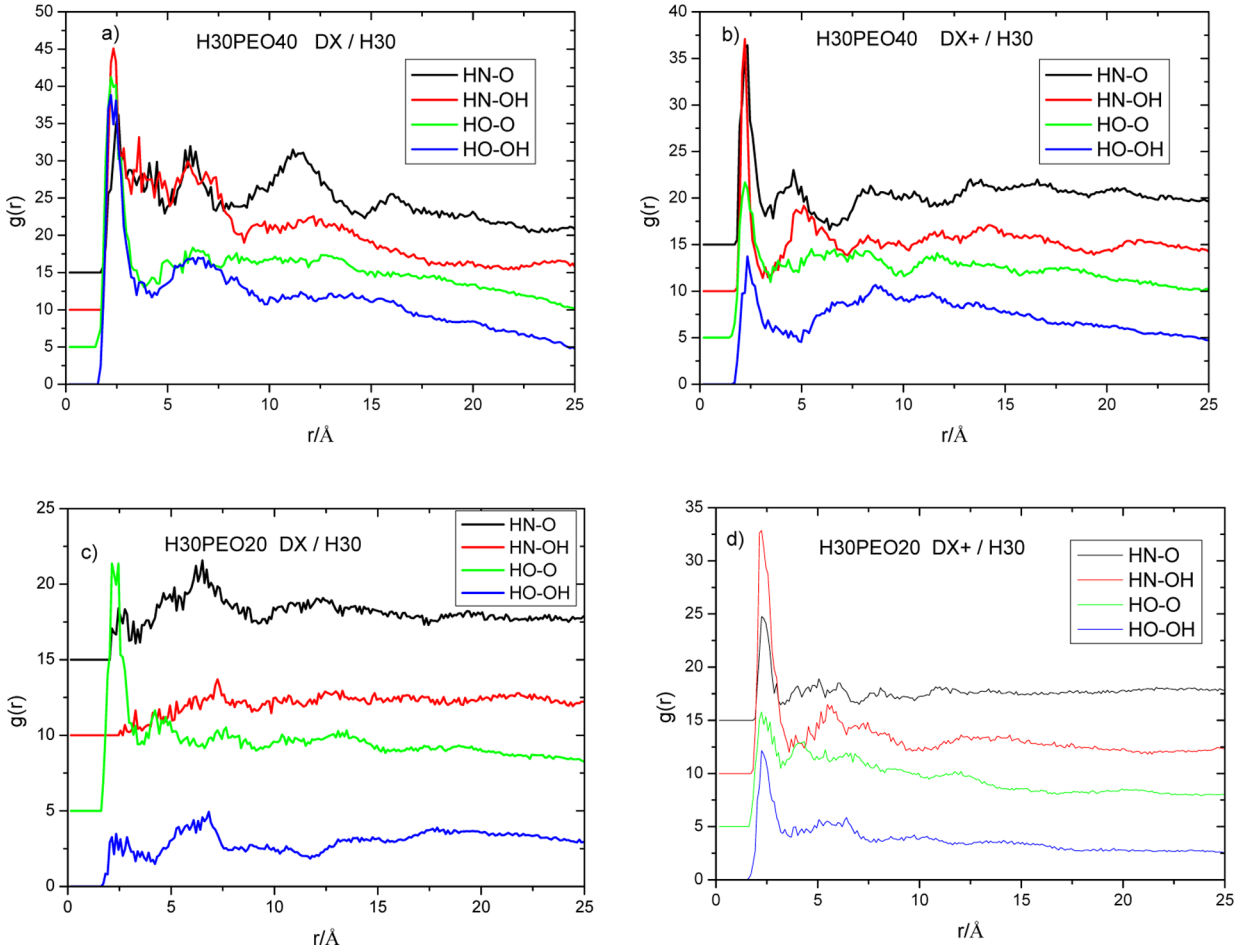

Figure 8. Pair correlation functions of characteristic hydrogen-bonding-capable pairs between doxorubicin and the polymeric host (HN−O, HN−OH, HO−O, HO−OH in order from top to bottom in the legends). Each correlation function is shifted in the *y*-axis by a constant factor of 5 with respect to the preceding curve, for clarity.

level of hydrogen bonding between the neutral drug molecules and water appears to be more suppressed in the H30PEO20 and H30PEO40 systems, as implied by the lower amplitude of the relevant peak in the radial distribution functions. A possible reason for that can be related to the antagonistic action of hydrogen bonding between the amine hydrogens of the drug and the polymeric moiety.

An analogous picture regarding the degree of hydrogen bonding between the drug molecules and the PEGylated polyester can be described by examining the hydrogen-bonding-capable atomic pairs between DOX and the polymeric nanoparticle, as shown in Figure 8.

For both the H30PEO20 and H30PEO40 systems, the protonated DOX molecules appear to form well-defined hydrogen bonds with the polymeric nanoparticle as indicated by the location (≅2.5 Å) and the intensity of the hydrogen-bonding peaks. For the charged drugs, the most frequent hydrogen-bonding pair (as implied by its relative intensity) is between the amine hydrogen of the drug (HN) and the hydroxyl oxygens of the polymer (OH). In the case of the neutral drug molecules, however, hydroxyl hydrogens (HO) seem to play the most significant role in hydrogen bonding with the polymer. The main difference when comparing the behavior between the systems including the two different polymeric particles is that in the shorter-PEG-arm system (H30PEO20) hydrogen bonding between the amine hydrogen of the neutral drugs and the polymeric host is rather suppressed. This might be related to the distinct conformations assumed by each

dx.doi.org/10.1021/jp312125c | J. Phys. Chem. B 2013, 117, 2564−2575

polymer, which might affect the availability of hydrogen-bonding-capable sites, e.g., by exposing them (in geometric terms) to a different degree to the drug's amine group.

III.2. Dynamic Aspects. The self-association between DOX molecules and their complexation with the polymeric particle are expected to affect significantly their transport properties and ultimately their biodistribution.[53] To assess such effects, we monitored the mean squared displacement (MSD) of the center of mass of the DOX molecules in the examined systems, as depicted in Figure 9.

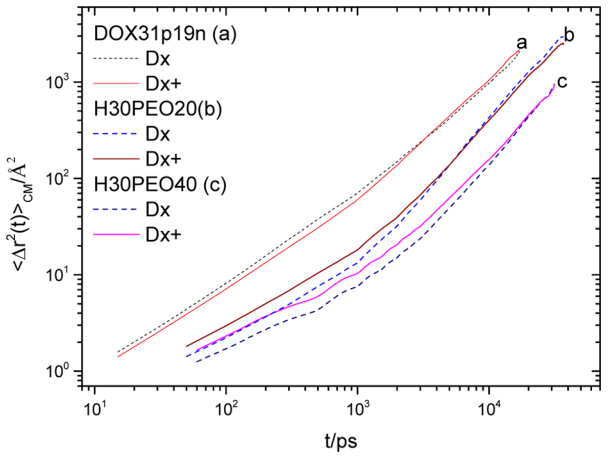

Figure 9. Mean squared displacement of the center of mass of the DOX molecules in DOX31p19n (a), H30PEO20 (b), and H30PEO40 (c).

Visual inspection of Figure 9 shows that the diffusive properties of the drug molecules depend sensitively on the presence of the polymeric host. Faster diffusion is observed in the polymer-free system (DOX31p19n), while the slower drug transport corresponds to the larger in size polymeric host. Even in the polymer-free system, however, due to the formation of drug clusters as discussed earlier, DOX diffusion is expected to be slower than that of a single drug molecule. A simple calculation of the expected diffusion coefficient (D_{ES}) of a single DOX molecule based on the Einstein–Stokes formula

$$D_{ES} = \frac{k_B T}{6\pi n R} \tag{3}$$

where n is the viscosity of the solvent (here for water is taken to be 1.002 cP) and R the hydrodynamic radius of a drug molecule (here we use as an approximate value that of the radius of gyration) renders a value of ≅1.7 mm^2/h. An estimation of the diffusion coefficient of the DOX molecules in system DOX31p19n based on the MSD behavior shown in Figure 7 (from curve a) via the expression

$$D = \lim_{t\to\infty} \frac{\langle \Delta r^2(t)\rangle_{CM}}{6t} \tag{4}$$

yields a value of $D \cong 0.60$ mm^2/h, which is about 3 times smaller compared to D_{ES} but in a good agreement with the estimation of $D \cong 0.57$ mm^2/h for the diffusion coefficient of free extracellular doxorubicin[54] and with that from *diffusion ordered spectroscopy* (DOSY) measurements,[44] $D \cong 0.59 \pm 0.21$ mm^2/h. If we consider, as demonstrated earlier, that, besides the DOX self-assembly in clusters, association with the polymeric host takes place as well, an even lower apparent diffusion coefficient can be rationalized. Indeed, a similar estimation of the diffusion coefficients of the DOX molecules in the polymer-containing systems via eq 4 yields values of $D \cong 0.47$ mm^2/h and $D \cong 0.15$ mm^2/h in the H30PEO20 and H30PEO40 systems, respectively. The observed dependence of the diffusion coefficient of the DOX molecules on the size of the polymeric host is consistent with the different average sizes of the two PEGylated polyesters, if the latter are viewed as diffusing particles possessing different hydrodynamic radii.

To obtain a more quantitative account of the self-diffusive dynamics of the DOX molecules in each of the examined systems, we have calculated the incoherent dynamic structure factor arising from the center of mass of the drug molecules, according to eq 5:

$$S_{inc}(q, t) = \left\langle \frac{1}{N} \langle \sum_{i=1}^{N} e^{-i\mathbf{q}[\mathbf{r}_i(t)-\mathbf{r}_i(0)]} \rangle_{|q|} \right\rangle_{\text{directions}} \tag{5}$$

where $\mathbf{q}$ is the scattering vector with magnitude q, N refers to the number of scatterers (here the number of DOX molecules), and $\mathbf{r}_i$ symbolizes the position vector of the ith scatterer. For the scattering vector magnitude q examined, we have averaged over 20 different directions randomly distributed on a sphere's surface in order to avoid effects associated with anisotropy of the distribution of the DOX molecules within the simulation box. $S_{inc}(q, t)$ probes density fluctuations due to the self-motion of the monitored scatterers, allowing both spatial and temporal resolution of their motion.[55] Figure 10 depicts the incoherent

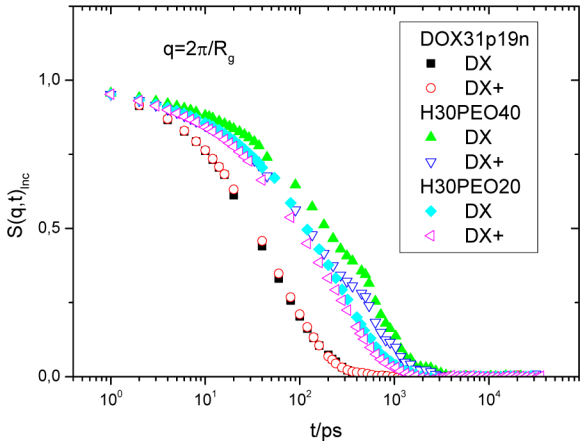

Figure 10. Incoherent dynamic structure factor arising from the self-motion of the centers of mass of the DOX molecules in the examined systems. The scattering vector magnitude corresponds to a length scale defined by the radius of gyration of the drug molecules.

dynamic structure factor for a q-magnitude describing a length scale representing the average size of a DOX molecule (≅4.8 Å), which is very close to the average distance between first neighbors within the drug clusters (see Figure 3).

A general observation is that the scattering functions decorrelate systematically with a slower rate (i.e., they reach zero at longer time scales) when moving from the polymer-free (H31p19n) to the smaller in size (H30PEO20) and finally to the larger in size (H30PEO40) polymeric host, while in the polymer-containing systems a somewhat faster decay is also observed for the protonated drugs compared to their neutral counterparts. Since the length scale probed is comparable to the distance between the first neighbors of the drug molecules,

dx.doi.org/10.1021/jp312125c | J. Phys. Chem. B 2013, 117, 2564–2575

the corresponding time scale is commensurate to that corresponding to the internal motion of DOX within the formed clusters. This time scale can be estimated by integrating the relevant correlation function, i.e., $\tau = \int_0^\infty S_{inc}(q, t)\, dt$. Table 2 presents the so calculated characteristic times.

Table 2. Average Times Characterizing the Individual Motion of the Protonated and Neutral Drug Molecules within the Formed Clusters

system	τ (ps, DX)	τ (ps, DX+)
DOX31p19n	62.5	65.2
H30PEO20	213.1	199.5
H30PEO40	434.4	350.7

According to the calculated values, the neutral drug molecules move within the clusters by more than 3.5 times in the H30PEO20 and about 7 times in the H30PEO40 slower compared to the polymer-free model, while these factors amount to about 3 and 5.4 times, respectively, for the charged drugs. Therefore, the individual motion of drug molecules within the clusters is considerably more constrained in the presence of the polymeric host compared to the polymer-free case, while the degree of confinement appears to increase with the size of the polymeric nanoparticle.

To get more information regarding the collective motion of the drug molecules and thus on the time scale associated with the longevity of the formed drug clusters, we have monitored the distinct Van Hove correlation function $G_d(r, t)$:[55]

$$G_d(r, t) = \frac{1}{N}\left\langle \sum_i \sum_{j\neq i} \delta[r - |\mathbf{r}_i(t) - \mathbf{r}_j(0)|] \right\rangle \quad (6)$$

N is the total number of particles (here the drug molecules each represented by its center of mass), δ is the Dirac's function, and $\mathbf{r}_i(t)$ is the position vector of the ith particle at time t. This function probes density fluctuations due to the collective motion of the examined particles at a length scale corresponding to a separation r between the particles and at a time scale t. At the time origin, $G_d(r, t = 0)$ is proportional to

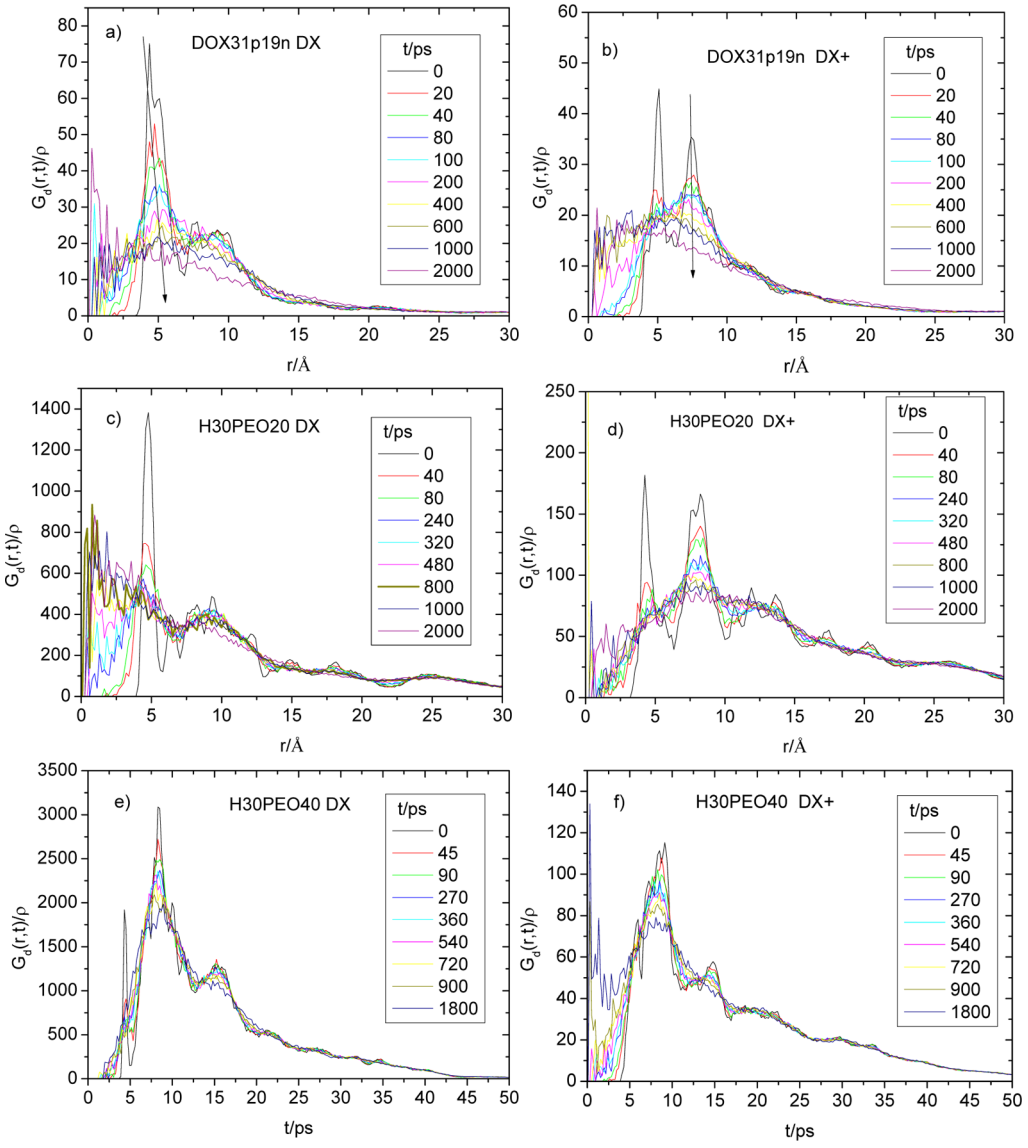

Figure 11. Distinct Van Hove correlation functions of the neutral (left column) and protonated (right) doxorubicin molecules. The arrows shown in the DOX31p19n spectra (a, b) point to the direction of increase of the time span. The same direction applies for the rest of the spectra as well.

dx.doi.org/10.1021/jp312125c | J. Phys. Chem. B 2013, 117, 2564−2575

the radial distribution function $g(r)$, $G_d(r, 0) = \rho g(r)$, where ρ represents the particles' number density. At large time spans and long separations, the position of each particle becomes uncorrelated to the initial position of a different particle, so that $G_d(r, t)$ tends to the average density of the particles in the system. Figure 11 illustrates the distinct van Hove correlation functions of the DOX molecules in the examined models.

A common feature characterizing all $G_d(r, t)$ spectra is that as time lapses the peaks corresponding to $t = 0$ (i.e., those shown previously in Figure 3) lose amplitude. This should be interpreted as a progressive "loss of memory" of the local structure with respect to the spatial distribution of DOX molecules at $t = 0$. In other words, the initial local arrangement of drug molecules around a central one progressively loses its coherence to the point that the final configuration becomes completely uncorrelated to the starting state. The longer it takes for a peak to be smeared out, the higher the persistency of the local structure it refers to. With this interpretation in mind, we can start following the spatial reorganization of the local assemblies of drug molecules as a function of time.

Focusing on the polymer-free model (Figure 11a and b), it appears that, for the neutral drugs (Figure 11a), both the first-neighbor and the second-neighbor peaks are smeared out at a time scale of several hundred ps. On the other hand, the same peaks describing the protonated drug molecules lose their amplitudes much faster. The main maximum close to $r \cong 5$ Å describing the first neighbors (Figure 11b) flattens at a time span of the order of a few tens of ps, while that describing the local arrangement of drug molecules at larger separations persists for at least a decade longer. In the H30PEO20 model, the time dependence of the amplitude of the peaks characterizing the charged DOX molecules is similar to that observed in the corresponding polymer-free case, while in the neutral drug spectra (Figure 11c) the first peak decays at a higher rate compared to its analogue in DOX31p19n (Figure 11a). The different rates characterizing the decay of the first and second neighbor peaks in Figure 11a–d imply that the second neighbor maximum in these systems does not arise from the existence of trimers or larger in size clusters, since in that case survival of larger in size clusters would essentially mean survival of dimers (within these larger clusters) as well.

In the system containing the longer-arm PEGylated polyester, no significant differences are noted when comparing the behavior of the charged to that of the neutral drug molecules (Figure 11e,f) as far as it concerns the decay rate of the amplitude of the observed peaks. In this model, irrespective of the charge of the drug molecules, the second-neighbor peak seems to be flattened at a time scale close to 2 ns, whereas the first neighbor peak loses its amplitude at a very slow rate, retaining most of its amplitude even at the longer time scale examined here (at even longer time scales, statistics become less reliable). This observation indicates that, in the H30PEO40 model, the collective rearrangement of the DOX molecules, particularly at length scales consistent with internal separations within the clusters, is much slower and therefore the structural characteristics of the formed assemblies are more persistent compared to the polymer-free case and to that of the smaller in size polymer nanoparticle.

IV. SUMMARY/CONCLUSIONS

In this work, we have examined by means of molecular dynamics simulations fully atomistic models of aqueous solutions of the anticancer drug doxorubicin in a polymer-free system and in the presence of a PEGylated hyperbranched polyester in physiological conditions of pH and at body temperature. By monitoring static and dynamic properties, we have been able to assess the effects of the presence of the polymer compound and of its structural characteristics (i.e., length of the PEG arms) in the clustering behavior of the neutral and charged drug molecules. It was found that DOX molecules self-organize in clusters of stacked molecules both in the polymer free system and in the presence of the PEGylated hyperbranched polyesters, but several differences were noted. The characteristics of the formed clusters (orientation of the drug molecules within a cluster, spatial distribution of the aggregates, individual and collective dynamics of the drug molecules, nature of the formed hydrogen bonds with the polymeric host) were found to depend on the structural features of the polymer compound. In addition, differences are observed in the structural organization of the aggregates between the charged and neutral molecules.

In more detail, the drug clusters (particularly those containing protonated drug molecules) are preferentially located close to the polymer's periphery. The internal structural characteristics of the formed clusters are drastically affected by the presence of the polymeric host and by its morphological details, while their spatial arrangement around the polymeric nanoparticle depends as well on the size of its PEG arms. Hydrogen bonding between drug and water is stronger in the protonated drugs and is promoted mainly via the hydrogens of the charged amine group in the sugar moiety. The same group also drives hydrogen bonding between the charged drugs and the polymer nanoparticle, while hydroxyl hydrogens of the drug contribute the most to hydroden bonding between the neutral DOX molecules and the polymeric compound. The hydrogen bonding pattern between the polymer and the drug shows also some differences in the two polymer-containing systems, probably related to the distinct conformations of the polymeric moiety originating from the different lengths of the PEG arms. From the dynamic point of view, transport properties of the DOX clusters are much slower in the polymer-containing systems as was anticipated, while their diffusional motion depends on the overall size of the polymeric nanoparticle, due to their association with the latter. This physical binding of the drug molecules to the polymer results in a characteristic slowing down of their individual motion with respect to the polymer-free case, by factors of at least 3 and 5 in the systems with the shorter and longer PEG arms, respectively. The individual translational motion of the drug molecules at a length scale comparable to their intracluster separation was found to be more restricted in the polymer-containing models while the structural coherence of the drug clusters was found to be more persistent in the system bearing the longer PEG arms.

The above-described results offer new insight on key experimental findings related to nanocarriers of DOX based on PEGylated hyperbranched polyesters.[23] The more effective clustering of DOX molecules in the presence of the polymeric nanoparticle with respect to the polymer-free case (i.e., via favorable enthalpic interactions with the nanocarrier and via geometric constriction within the nanoparticle's volume) results in a higher local concentration of the drug molecules and is consistent with the more effective therapeutic action observed experimentally when the drug is complexed with these nanoparticles.[23] In addition, the morphological details of the polymeric compound affect the clustering behavior of the drug molecules, leading potentially to a better control of their

dx.doi.org/10.1021/jp312125c | J. Phys. Chem. B 2013, 117, 2564–2575

pharmacological behavior. Namely, in the case of the systems studied, the hyperbranched polymer bearing longer PEG arms (and thus characterized by a higher PEG surface density), promotes the formation of more structurally coherent drug clusters which are kept physically bound to the nanoparticle's surface, increasing thus the probability for a more efficient transport of the drug molecules to the targeted site and for more favorable release profiles. On these grounds, increase of the efficiency of the drug loading and the targeted delivery of DOX when using even longer PEG arms can be envisaged, but it should be kept in mind that for an optimal performance of the polymeric nanocarrier in the effective drug binding and delivery, a balance must be retained as far as it concerns the drug/polymer binding and the tendency for aggregation between the formed polymer/drug complexes which may affect the efficiency of the transport to the targeted location and the final release profiles.[23]

The above-described associative behavior of the doxorubicin molecules is expected to be similar to that anticipated from other drugs belonging in the anthracycline family (e.g., epiadriamycin, daunomycin, etc.) and therefore may constitute the basis for the interpretation of relevant experimental observations in other members of that family or even utilized as a tool for the design of similar nonovectors and for the prediction of their behavior under analogous thermodynamic conditions.

■ ASSOCIATED CONTENT

Supporting Information

Snapshots of the systems after equilibration with visible water molecules and time correlation functions for the fluctuations of squared fluctuations of the radius of gyration of the PEGylated hyperbranched polysters. This material is available free of charge via the Internet at http://pubs.acs.org.

■ AUTHOR INFORMATION

Corresponding Author

*E-mail: karatas@eng.auth.gr. Phone: +302310995850.

Notes

The authors declare no competing financial interest.

■ ACKNOWLEDGMENTS

The author would like to thank Dr. A. Vargiu (Officina dei Materiali del CNR, UOS SLACS, and Dipartimento di Fisica, Università degli Studi di Cagliari, Monserrato, Italy) for providing the parameters and the initial structure of doxorubicin. This work was performed in the framework of the ESF COST action TD0802 "Dendrimers in Biomedical Applications". Part of this work was carried out under the HPC-Europa 2 project (CINECA Supercomputing Center, Bologna, Italy), funded by the European Commission—DG Research in the 7th Framework Program (Grant agreement no 228398).

■ REFERENCES

(1) Wang, A. Z.; Langer, R.; Farokhzad, O. C. Nanoparticle Delivery of Cancer Drugs. *Annu. Rev. Med.* **2012**, *63*, 185−198.

(2) Liu, X.; Rocchi, P.; Peng, L. Dendrimers as Non-Viral Vectors for siRNA Delivery. *New J. Chem.* **2012**, *36*, 256−263.

(3) Liu, X.; Liu, C.; Laurini, E.; Posocco, P.; Pricl, S.; Qu, F.; Rocchi, P.; Peng, L. Efficient Delivery of Sticky siRNA and Potent Gene Silencing in a Prostate Cancer Model Using a Generation 5 Triethanolamine-Core PAMAM Dendrimer. *Mol. Pharm.* **2011**, *9*, 470−481.

(4) Tanis, I.; Karatasos, K. Association of a Weakly Acidic Anti-Inflammatory Drug (Ibuprofen) with a Poly(amidoamine) Dendrimer as Studied by Molecular Dynamics Simulations. *J. Phys. Chem. B* **2009**, *113*, 10984−10993.

(5) Khandare, J.; Calderon, M.; Dagia, N. M.; Haag, R. Multifunctional Dendritic Polymers in Nanomedicine: Opportunities and Challenges. *Chem. Soc. Rev.* **2012**, *41*, 2824−2848.

(6) Ortega, P.; Cobaleda, B. M.; Hernandez-Ros, J. M.; Fuentes-Paniagua, E.; Sanchez-Nieves, J.; Tarazona, M. P.; Copa-Patino, J. L.; Soliveri, J.; de la Mata, F. J.; Gomez, R. Hyperbranched Polymers versus Dendrimers Containing a Carbosilane Framework and Terminal Ammonium Groups as Antimicrobial Agents. *Org. Biomol. Chem.* **2011**, *9*, 5238−5248.

(7) Paleos, C. M.; Tsiourvas, D.; Sideratou, Z.; Tziveleka, L.-A. Drug Delivery Using Multifunctional Dendrimers and Hyperbranched Polymers. *Expert Opin. Drug Delivery* **2010**, *7*, 1387−1398.

(8) Yates, C. R.; Hayes, W. Synthesis and Applications of Hyperbranched Polymers. *Eur. Polym. J.* **2004**, *40*, 1257−1281.

(9) Kontogiannopoulos, K. N.; Assimopoulou, A. N.; Hatziantoniou, S.; Karatasos, K.; Demetzos, C.; Papageorgiou, V. P. Chimeric Advanced Drug Delivery Nano Systems (chi-aDDnSs) for Shikonin Combining Dendritic and Liposomal Technology. *Int. J. Pharm.* **2012**, *422*, 381−389.

(10) Zhou, Y.; Huang, W.; Liu, J.; Zhu, X.; Yan, D. Self-Assembly of Hyperbranched Polymers and Its Biomedical Applications. *Adv. Mater.* **2010**, *22*, 4567−4590.

(11) Malmström, E.; Johansson, M.; Hult, A. Hyperbranched Aliphatic Polyesters. *Macromolecules* **1995**, *28*, 1698−1703.

(12) Chen, S.; Zhang, X.-Z.; Cheng, S.-X.; Zhuo, R.-X.; Gu, Z.-W. Functionalized Amphiphilic Hyperbranched Polymers for Targeted Drug Delivery. *Biomacromolecules* **2008**, *9*, 2578−2585.

(13) Kontoyianni, C.; Sideratou, Z.; Theodossiou, T.; Tziveleka, L.-A.; Tsiourvas, D.; Paleos, C. M. A Novel Micellar Pegylated Hyperbranched Polyester as a Prospective Drug Delivery System for Paclitaxel. *Macromol. Biosci.* **2008**, *8*, 871−881.

(14) Lee, H.; Larson, R. G. Molecular Dynamics Study of the Structure and Interparticle Interactions of Polyethylene Glycol-Conjugated PAMAM Dendrimers. *J. Phys. Chem. B* **2009**, *113*, 13202−13207.

(15) Lee, H.; Larson, R. G. Effects of Pegylation on the Size and Internal Structure of Dendrimers: Self-Penetration of Long PEG Chains into the Dendrimer Core. *Macromolecules* **2011**, *44*, 2291−2298.

(16) Lee, H.; Larson, R. G. Membrane Pore Formation Induced by Acetylated and Polyethylene Glycol-Conjugated Polyamidoamine Dendrimers. *J. Phys. Chem. C* **2011**, *115*, 5316−5322.

(17) Perstorp, http://www.perstorp.com/.

(18) Minko, T.; Batrakova, E. V.; Li, S.; Li, Y. L.; Pakunlu, R. I.; Alakhov, V. Y.; Kabanov, A. V. Pluronic block copolymers alter apoptotic signal transduction of doxorubicin in drug-resistant cancer cells. *J. Controlled Release* **2005**, *105*, 269−278.

(19) Wang, Y. J.; Bansal, V.; Zelikin, A. N.; Caruso, F. Templated Synthesis of Single-Component Polymer Capsules and Their Application in Drug Delivery. *Nano Lett.* **2008**, *8*, 1741−1745.

(20) Lüpertz, R.; Wätjen, W.; Kahl, R.; Chovolou, Y. Dose- and Time-Dependent Effects of Doxorubicin on Cytotoxicity, Cell Cycle and Apoptotic Cell Death in Human Colon Cancer Cells. *Toxicology* **2010**, *271*, 115−121.

(21) Chaudhary, A.; Nagaich, U.; Gulati, N.; Sharma, V. K.; Khosa, R. L. Enhancement of Solubilization and Bioavailability of Poorly Soluble Drugs by Physical and Chemical Modifications: A Recent Review. *J. Adv. Pharm. Technol. Res.* **2012**, *2*, 32−67.

(22) Zhang, H.; Dong, Y.; Wang, L.; Wang, G.; Wu, J.; Zheng, Y.; Yang, H.; Zhu, S. Low Swelling Hyperbranched Poly(amine-ester) Hydrogels for pH-Modulated Differential Release of Anticancer Drugs. *J. Mater. Chem.* **2011**, *21*, 13530.

(23) Zeng, X.; Zhang, Y.; Wu, Z.; Lundberg, P.; Malkoch, M.; Nyström, A. M. Hyperbranched Copolymer Micelles as Delivery

Vehicles of Doxorubicin in Breast Cancer Cells. *J. Polym. Sci., Part A: Polym. Chem.* **2012**, *50*, 280−288.
(24) Zou, J. H.; Shi, W. F.; Wang, J.; Jun, B. Encapsulation and Controlled Release of a Hydrophobic Drug Using a Novel Nanoparticle-Forming Hyperbranched Polyester. *Macromol. Biosci.* **2005**, *5*, 662−668.
(25) Gan, Z.; Jim, T. F.; Li, M.; Yuer, Z.; Wang, S.; Wu, C. Enzymatic Biodegradation of Poly(ethylene oxide-b-ε-caprolactone) Diblock Copolymer and Its Potential Biomedical Applications. *Macromolecules* **1999**, *32*, 590−594.
(26) Albertsson, A. C.; Karlsson, S. Degradable Polymers for the Future. *Acta Polym.* **1995**, *46*, 114−123.
(27) Gillies, E. R.; Frechet, J. M. J. Designing Macromolecules for Therapeutic Applications: Polyester Dendrimer-poly(ethylene oxide) "Bow-Tie" Hybrids with Tunable Molecular Weight and Architecture. *J. Am. Chem. Soc.* **2002**, *124*, 14137−14146.
(28) Eksborg, S. Extraction of Daunorubicin and Doxorubicin and Their Hydroxyl Metabolites: Self-Association in Aqueous Solution. *J. Pharmaceut. Sci.* **1978**, *67*, 782−785.
(29) Po, H. N.; Senozan, N. M. The Henderson-Hasselbalch Equation: Its History and Limitations. *J. Chem. Educ.* **2001**, *78*, 1499−1503.
(30) Dalmark, M.; Johansen, P. Molecular Association between Doxorubicin (Adriamycin) and DNA-Derived Bases, Nucleosides, Nucleotides, Other Aromatic Compounds, and Proteins in Aqueous Solution. *Mol. Pharmacol.* **1982**, *22*, 158−165.
(31) Tanis, I.; Karatasos, K.; Assimopoulou, A. N.; Papageorgiou, V. P. Modeling of Hyperbranched Polyesters as Hosts for the Multifunctional Bioactive Agent Shikonin. *Phys. Chem. Chem. Phys.* **2011**, *13*, 10808−10817.
(32) Schulz, R.; Vargiu, A. V.; Collu, F.; Kleinekathöfer, U.; Ruggerone, P. Functional Rotation of the Transporter AcrB: Insights into Drug Extrusion from Simulations. *PLoS Comput. Biol.* **2010**, *6*, e1000806.
(33) Wang, J.; Wolf, R. M.; Caldwell, J. W.; Kollman, P. A.; Case, D. A. Development and Testing of a General Amber Force Field. *J. Comput. Chem.* **2004**, *25*, 1157−1174.
(34) Weiner, S. J.; Kollman, P. A.; Nguyen, D. T.; Case, D. A. An All Atom Force Field for Simulations of Proteins and Nucleic Acids. *J. Comput. Chem.* **1986**, *7*, 230−252.
(35) Tanis, I.; Tragoudaras, D.; Karatasos, K.; Anastasiadis, S. H. Molecular Dynamics Simulations of a Hyperbranched Poly(ester amide): Statics, Dynamics, and Hydrogen Bonding. *J. Phys. Chem. B* **2009**, *113*, 5356−5368.
(36) Vargiu, A. V.; Collu, F.; Schulz, R.; Pos, K. M.; Zacharias, M.; Kleinekathöfer, U.; Ruggerone, P. Effect of the f610a Mutation on Substrate Extrusion in the AcrB Transporter: Explanation and Rationale by Molecular Dynamics Simulations. *J. Am. Chem. Soc.* **2011**, *133*, 10704−10707.
(37) Tanis, I.; Karatasos, K. Molecular Dynamics Simulations of Polyamidoamine Dendrimers and Their Complexes with Linear Poly(ethyleneoxide) at Different pH Conditions: Static Properties and Hydrogen Bonding. *Phys. Chem. Chem. Phys.* **2009**, *11*, 10017−10028.
(38) Jorgensen, W. L.; Chandrasekhar, J.; Madura, J. D.; Impey, R. W.; Klein, M. Comparison of Simple Potential Functions for Simulating Liquid Water. *J. Chem. Phys.* **1983**, *79*, 926−935.
(39) Benková, Z.; Szefczyk, B.; D. S. Cordeiro, M. N. l. Molecular Dynamics Study of Hydrated Poly(ethylene oxide) Chains Grafted on Siloxane Surface. *Macromolecules* **2011**, *44*, 3639−3648.
(40) Humphrey, W.; Dalke, A.; Schulten, K. VMD - Visual Molecular Dynamics. *J. Mol. Graphics* **1996**, *14*, 33−38.
(41) Feller, S. E.; Zhang, Y.; Pastor, R. W.; Brooks, B. R. Constant Pressure Molecular Dynamics Simulation: the Langevin Piston Method. *J. Chem. Phys.* **1995**, *103*, 4613−4621.
(42) Darden, T.; Perera, L.; Li, L.; Pedersen, L. New Tricks for Modelers from the Crystallography Toolkit: the Particle Mesh Ewald Algorithm and Its Use in Nucleic Acid Simulations. *Structure* **1999**, *7*, R55−R60.
(43) Phillips, J.; Braun, R.; Wang, W.; Gumbart, J.; Tajkhorshid, E.; Villa, E.; Chipot, C.; Skeel, R.; Kale, L.; Schulten, K. Scalable Molecular Dynamics with NAMD. *J. Comput. Chem.* **2005**, *26*, 1781−1782.
(44) Agrawal, P.; Barthwal, S. K.; Barthwal, R. Studies on Self-Aggregation of Anthracycline Drugs by Restrained Molecular Dynamics Approach Using Nuclear Magnetic Resonance Spectroscopy Supported by Absorption, Fluorescence, Diffusion Ordered Spectroscopy and Mass Spectrometry. *Eur. J. Med. Chem.* **2009**, *44*, 1437−1451.
(45) Davies, D. B.; Veselkov, D. A.; Evstigneev, M. P.; Veselkov, A. N. Self-Association of the Antitumour Agent Novatrone (Mitoxantrone) and Its Hetero-Association with Caffeine. *J. Chem. Soc., Perkin Trans. 2* **2001**, 61−67.
(46) Evstigneev, M. P.; Khomich, V. V.; Davies, D. B. Self-Association of Daunomycin Antibiotic in Various Buffer Solutions. *Russ. J. Phys. Chem.* **2006**, *80*, 741−746.
(47) Posocco, P.; Ferrone, M.; Fermeglia, M.; Pricl, S. Binding at the Core. Computational Study of Structural and Ligand Binding Properties of Naphthyridine-Based Dendrimers. *Macromolecules* **2007**, *40*, 2257−2266.
(48) Beezer, A. E.; King, A. S. H.; Martin, I. K.; Mitchel, J. C.; Twyman, L. J.; Wain, C. F. Dendrimers as Potential Drug Carriers; Encapsulation of Acidic Hydrophobes within Water Soluble PAMAM Derivatives. *Tetrahedron* **2003**, *59*, 3873−3880.
(49) Astruc, D.; Boisselier, E.; Ornelas, C. Dendrimers Designed for Functions: from Physical, Photophysical, and Supramolecular Properties to Applications in Sensing, Catalysis, Molecular Electronics, Photonics, and Nanomedicine. *Chem. Rev.* **2010**, *110*, 1857−1959.
(50) Lee, H.; Baker, J. R.; Larson, R. G. Molecular Dynamics Studies of the Size, Shape, and Internal Structure of 0% and 90% Acetylated Fifth-Generation Polyamidoamine Dendrimers in Water and Methanol. *J. Phys. Chem. B* **2006**, *110*, 4014−4019.
(51) Chiessi, E.; Cavalieri, F.; Paradossi, G. Water and Polymer Dynamics in Chemically Cross-Linked Hydrogels of Poly(vinyl alcohol): a Molecular Dynamics Simulation Study. *J. Phys. Chem. B* **2007**, *111*, 2820−2827.
(52) Jeffrey, G. A.; Saenger, W. *Hydrogen Bonding in Biological Structures*; Springer-Verlag: Berlin, 1991.
(53) Speelmans, G.; Staffhorst, R. W. H. M.; de Kruijff, B.; de Wolf, F. A. Transport Studies of Doxorubicin in Model Membranes Indicate a Difference in Passive Diffusion across and Binding at the Outer and Inner Leaflet of the Plasma Membrane. *Biochemistry* **1994**, *33*, 13761−13768.
(54) Eikenberry, S. A Tumor Cord Model for Doxorubicin Delivery and Dose Optimization in Solid Tumors. *Theor. Biol. Med. Modell.* **2009**, *6*, 1−20.
(55) Hansen, J.-P.; McDonald, I. R. *Theory of Simple Liquids*, 3rd ed.; Elsevier: Amsterdam, The Netherlands, 2006.